ARTICLES

Multidimensional classical Liouville dynamics with quantum initial conditions

Illia Horenko, Burkhard Schmidt,[a] and Christof Schütte
Freie Universität Berlin, Institute for Mathematics II, Arnimallee 2–6, D–14195 Berlin, Germany

(Received 18 April 2002; accepted 13 June 2002)

A simple and numerically efficient approach to Wigner transforms and classical Liouville dynamics in phase space is presented. (1) The Wigner transform can be obtained with a given accuracy by optimal decomposition of an initial quantum-mechanical wave function in terms of a minimal set of Gaussian wave packets. (2) The solution of the classical Liouville equation within the locally quadratic approximation of the potential energy function requires a representation of the density in terms of an ensemble of narrow Gaussian phase-space packets. The corresponding equations of motion can be efficiently solved by a modified leap-frog integrator. For both problems the use of Monte Carlo based techniques allows numerical calculation in multidimensional cases where grid-based methods such as fast Fourier transforms are prohibitive. In total, the proposed strategy provides a practical and efficient tool for classical Liouville dynamics with quantum-mechanical initial states. © *2002 American Institute of Physics.* [DOI: 10.1063/1.1498467]

I. INTRODUCTION

The classical Liouville equation (CLE) represents the conceptually most straightforward approach to the classical approximation of quantum dynamics. Usually the time evolution of the wave function or density matrix of a quantum-mechanical system is expressed in terms of the time-dependent Schrödinger equation or the quantum Liouville equation (QLE), respectively. Employing the technique of Wigner transforms, these equations can be cast into phase space. Then the $\hbar \to 0$ limit of the corresponding equation of motion directly yields the CLE describing the dynamical behavior of a classical (quasi-) distribution function at constant energy in phase space.[1–4] If, in addition, the distribution is approximated by deltalike points in phase space, the dynamics is governed by Newton's or Hamilton's equations of motion which are routinely solved in classical molecular dynamics simulations.

Recently, the interest in the numerical treatment of the CLE has been renewed in the context of a mixed quantum-classical approach to molecular dynamics. The quantum-classical Liouville equation (QCLE) has been derived as a first order approximation to the partial Wigner transform of full quantum dynamics.[5–10] This equation describes the evolution of the multistate dynamics of a molecular system including nonadiabatic transitions. In particular, when the QCLE is solved by a Trotter splitting of the quantum-classical Liouville operator, one of the propagators represents purely classical Liouville dynamics along each of the adiabatic potential energy surfaces of the quantum subsystem.[11–14]

The solution of the CLE for multidimensional problems such as typically encountered in molecular dynamics presents a formidable challenge. There are two principle difficulties which shall be dealt with in the present work. First of all, the classical propagation in time requires a solution of a partial differential equation for a continuous distribution function in classical phase space. A direct numerical solution employing, e.g., fast Fourier transforms is prohibitive for increasing dimensionality. Instead, the ubiquituous trajectory approach employs Monte Carlo sampling of the phase-space distribution by deltalike points and propagation of the corresponding trajectories. However, the discrete sampling may have severe limitations where faithful, i.e., smooth representations are required. This is of crucial importance, e.g., for the nonadiabatic population exchange in QCLE dynamics.[13] Other examples are found in statistical mechanics if multidimensional potential energy surfaces with high barriers are to be sampled efficiently.[15] Yet another application is the evaluation of nonclassical forces occurring in the ''Bohmian'' formulation of quantum mechanics.[16]

The second major problem in CLE dynamics stems from the generation of the initial conditions. Even though the dynamics may be treated within the classical approximation, there is a wide class of applications where the quantum nature of the initial state is of importance. A typical numerical realization of classical molecular dynamics with quantum initial conditions is the quasiclassical trajectory (or Wigner trajectory) method where the initial conditions of a classical trajectory simulation are chosen according to an initial quantum density. Such an approach is frequently used to describe (reactive) molecular collisions.[17] Other applications are in the field of photoinduced processes, e.g., molecular photodissociation dynamics.[18,19] In such cases the initial distribution function has to be calculated as a Wigner transform of the

[a]Author to whom correspondence should be addressed. Electronic mail: burkhard@math.fu-berlin.de

initial quantum-mechanical wave function or density. Again, a direct numerical implementation of the Wigner transform employing Fourier transforms is computationally not feasible for higher dimensionality. The alternative of calculating the Wigner distribution function directly appears to be numerically even more cumbersome.[20–22] Hence, the vast majority of existing quasiclassical numerical studies of (photoinduced) reaction dynamics has been limited to the case of initial states of Gaussian shape thus excluding interesting quantum effects connected with delocalized initial molecular states, e.g., of vibrationally or rotationally excited states. In such cases the quantum-mechanical nature of the initial state is reflected in negative values of the Wigner (quasi-) distribution function in certain regions of phase space.[23]

The present work aims at developing efficient numerical schemes for use in classical Liouville dynamics with quantum initial conditions that are not limited to low dimensionality. Both problems mentioned above can be solved in an efficient way by the use of Gaussian bell functions. Such basis sets have been successfully applied to a variety of problems in theoretical chemistry or molecular physics. For example, Gaussian basis sets are routinely used for quite some time to compute the electronic structure of molecular systems even though they do not even constitute a natural basis for such problems.[24] Furthermore, Gaussian wave packets (GWPs) have been used for the numerical solution of the Schrödinger equation for the nuclear motion of molecules. This includes both the calculation of stationary vibrational wave functions[25,26] and the description of wave packet dynamics of photochemical or photophysical processes.[27–30] The phase-space equivalent to GWPs are Gaussian phase-space packets (GPPs) which are obtained as Wigner transforms of GWPs. Indeed, there are first indications that GPPs can be used to efficiently solve the CLE.[15,31] Moreover, GPPs were recently demonstrated by the present authors to serve as a convenient representation of densities and coherences evolving under the QCLE.[13]

The remainder of the paper is organized as follows: In Sec. II we propose a Monte Carlo based technique to decompose a wave function in terms of a minimal set of multidimensional GWPs. The resulting initial Wigner distribution functions are expressed in terms of GPPs. Subsequently, in Sec. III we present equations of motion and a numerical propagator for GPP–based classical Liouville dynamics. An application to photodissociation dynamics illustrates the use of the proposed schemes. Finally, Sec. IV contains our conclusions.

II. INITIAL QUANTUM CONDITIONS

A. GWP representation of wave function

As a prerequisite to the Wigner transformation, the initial wave function has to cast into a suitable representation. Hence, the first step of the proposed strategy consists of fitting a minimal number of multidimensional GWPs to the initial quantum-mechanical wave function. We use the standard definition for complex-valued GWPs in D dimensional position space

$$\psi_j(R)=A_j \exp\left[-(R-R_j)^T a_j (R-R_j)+\frac{i}{\hbar}P_j^T(R-R_j)\right] \tag{1}$$

with real amplitudes $A_j \in \mathcal{R}$ and where the expectation values $R_j, P_j \in \mathcal{R}^D$ give the centers of the wave packets in position and momentum space, respectively. The symmetric, positively definite matrices $a_j \in \mathcal{R}^{D\times D}$ specify the shape of the wave packet. Without loss of generality it is also possible to restrict the above ansatz to the use of diagonal matrices a_j, i.e., to represent the wave function in terms of spherically symmetric GWPs. The error functional

$$\Phi(N;\psi_j)=\int_{\mathcal{R}^D} dR \left|\Psi(R)-\sum_{j=1}^{N}\psi_j(R)\right|^2 \tag{2}$$

characterizes the deviation of the initial wave function $\Psi(R)$ from a linear superposition of GWPs. It has to be minimized with respect to the number N of GWPs and the parameters R_j, P_j, A_j, a_j. In practice, the minimization is based on a Monte Carlo technique to solve the multidimensional integral in Eq. (2). For a given ϵ as an upper limit of Φ, the following algorithm is suggested:

(1) Randomly choose a set of points in coordinate space where the wave function significantly differs from zero.
(2) $N=1$: Pick the initial value R_1 for the position of the center of the first GWP from the above-mentioned set.
(3) Minimize the error Φ with respect to the parameters R_j, P_j, A_j, a_j for $j=1,\ldots,N$. In principle this can be done by means of any standard minimization routine. In our case we used the Nelder–Mead scheme due to good convergence characteristics.[32]
(4) If the resulting value for the error Φ still remains greater than ϵ, increase the number N by one. The initial value for the position of the newly added GWP is chosen to be the point of maximal deviation of the linear combination of GWPs from the above-mentioned set of Monte Carlo points sampling the exact wave function, see step (1).
(5) Redo the minimization [steps (3)–(4)] until the desired accuracy is reached ($\Phi<\epsilon$).

We demonstrate the use of the decomposition of wave functions in terms of GWPs for two standard examples, a harmonic oscillator and a Morse oscillator supporting 16 vibrational states resembling the potential energy function of molecular hydrogen. Figure 1 shows the number of GWPs needed to represent bound state wave functions with an error $\Phi<\epsilon=0.01$. It is found that—apart from fluctuations due to the Monte Carlo procedure—the number N of GWPs grows linearly with the vibrational quantum number v, even for the strongly anharmonic wave functions of the Morse oscillator near the dissociation limit. The decomposition itself is illustrated in Fig. 2 for the $v=4$ state of the harmonic and Morse oscillator. Note that in general there is no simple one–to–one correspondence between the number N of GWPs and the number of lobes, $v+1$, of the wave function. For example, we find $N=v$ for the harmonic wave function in the upper panel of Fig. 2. It is emphasized that the above algorithm represents the wave function using a minimal number of

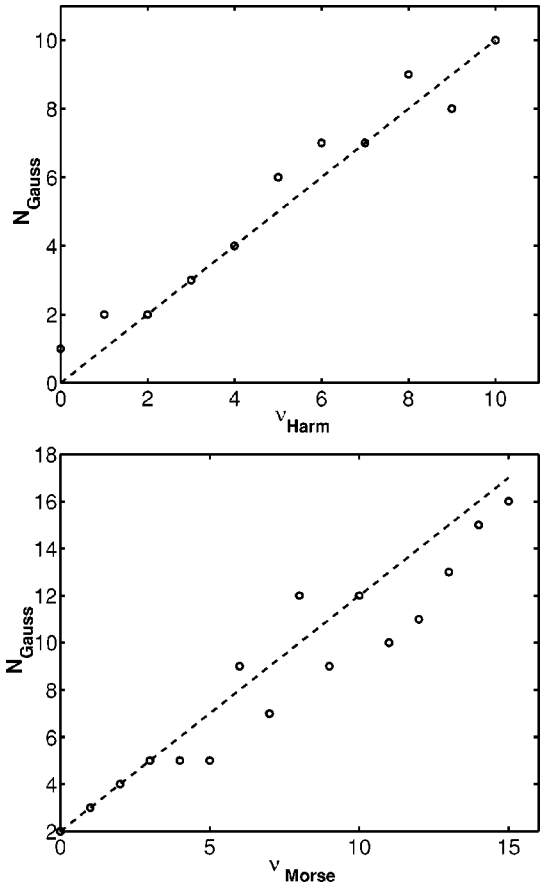

FIG. 1. Number of Gaussian wave packets in decomposition (2) of bound state wave function vs vibrational quantum number ($\epsilon=0.01$). Upper: Harmonic oscillator. Lower: Morse oscillator.

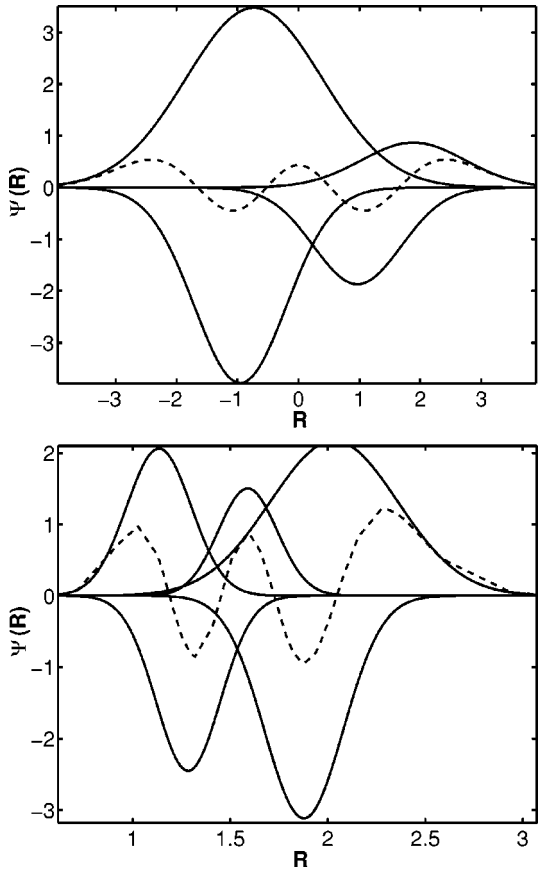

FIG. 2. Decomposition of $v=4$ bound state wave function (dashed) in terms of N Gaussian wave packets (solid). Upper: Harmonic oscillator with $N=4$. Lower: Morse oscillator with $N=5$.

GWPs which is instrumental for the calculation of the Wigner transform described in the following.

B. Wigner transform of wave function

In the following we assume that a decomposition of a wave function $\Psi(R)$ in terms of a sum of GWPs, i.e., a set of parameters $(R_j,P_j,A_j,a_j,j=1\ldots N)$ such that $\Phi<\epsilon$ in Eq. (2) is given. Then the Wigner distribution corresponding to the original wave function $\Psi(R)$ can be approximated by the Wigner distribution obtained from the linear superposition of GWPs,

$$W(R,P)=\frac{1}{(2\pi\hbar)^D}\int_{\mathcal{R}^D} dS\,\Psi^*\left(R+\frac{S}{2}\right)\Psi\left(R-\frac{S}{2}\right)\times\exp\left(-\frac{i}{\hbar}P^TS\right)$$
$$=\sum_j W_j(R,P)+\sum_{j<k} W_{jk}(R,P)+\mathcal{O}(\epsilon). \tag{3}$$

The terms in the single sum stand for the Wigner transforms of the individual GWPs of Eq. (1) which simply result in products of Gaussians in R and P,

$$W_j(R,P)=\frac{|A_j|^2}{(\sqrt{2\pi}\hbar)^D\sqrt{\det E_j}}\exp\left[-2(R-R_j)^Ta_j(R-R_j)-\frac{1}{2\hbar^2}(P-P_j)^TE_j^{-1}(P-P_j)\right], \tag{4}$$

where E_j stands for a diagonal matrix containing the eigenvalues of a_j. Note that these are known to be the only cases of positive definite Wigner distributions.[23] In contrast, the terms in the double sum are due to the coherence of different GWPs,

$$W_{jk}(R,P)=\frac{2A_jA_k}{(\sqrt{2\pi}\hbar)^D\sqrt{\det J_{jk}}}\times\exp[-b_{jk}+\tfrac{1}{2}d_{jk}^TJ_{jk}^{-1}d_{jk}-\tfrac{1}{2}e_{jk}^TJ_{jk}^{-1}e_{jk}]\times\cos[-c_{jk}+d_{jk}^TJ_{jk}^{-1}e_{jk}], \tag{5}$$

where J_{jk} is the diagonal matrix containing the eigenvalues of $(a_j+a_k)/2$ and where the following abbreviations have been used:

$$b_{jk}=(R-R_j)^Ta_j(R-R_j)+(R-R_k)^Ta_k(R-R_k),$$
$$c_{jk}=\frac{1}{\hbar}(P_j^T(R-R_j)-P_k^T(R-R_k)),$$
$$d_{jk}=-a_j(R-R_j)+a_k(R-R_k), \tag{6}$$

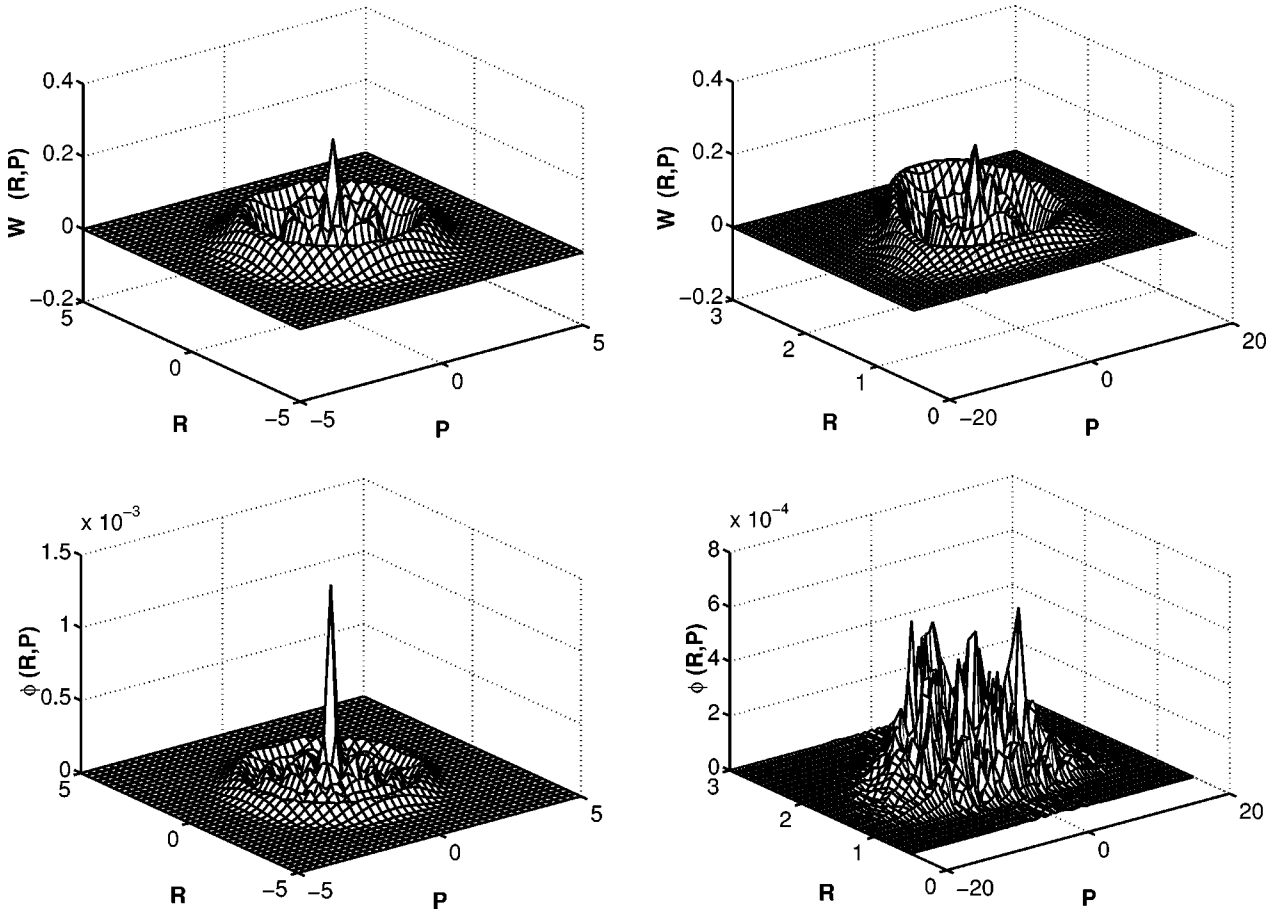

FIG. 3. Upper: Wigner-transform of the Gauss-decomposed $v=4$ vibrational eigenfunction for harmonic (left) and Morse (right) oscillator using $N=4$ or $N=5$ Gaussian wave packets, respectively (see also Figs. 1 and 2). Lower: Corresponding local quadratical differences from known analytical results for harmonic (left) and Morse (right) oscillator.

$$e_{jk}=\frac{1}{\hbar}\left(P-\frac{P_j-P_k}{2}\right).$$

Note that the cos function in (5) can take negative values thus indicating the nonclassical nature of the coherences. In particular, Eq. (3) reduces to a ''Schrödinger cat state'' in the case of only two GWPs which can be thought of as a phase-space analogue for a coherent superposition state of a two-level system. The contribution of the coherence to the corresponding quasidistribution function is a third Gaussian at the midpoint of the line joining the centers (R_1,P_1) and (R_2,P_2) but with a cos-type modulation in the direction perpendicular to that line.[4,33]

Wigner distribution functions for the two examples introduced above (harmonic and Morse oscillator) are illustrated in Fig. 3. Despite of the relatively complex shape of the distribution $W(R,P)$, the analytically known Wigner distributions of the harmonic and Morse oscillator[34,35] can be reproduced with a local error of less than 10^{-3} using only 10 or 15 terms in the double sum of Eq. (3), respectively.

C. GPP representation of Wigner function

Once the analytical expression (3) for the initial Wigner distribution function is available, the next step is to express it in a way that is suitable for numerical solution of the classical Liouville equation (CLE) as described in the next section. In the same spirit as the decomposition of the wave function in terms of GWPs described above, we use Gaussian phase-space packets (GPPs) similar to those in Eq. (4) to express the Wigner distribution function. However, the strategy has to be slightly different. While we are trying to minimize the number of GWPs in the representation of the initial wave function in order to reduce the computational effort to evaluate the double sum in Eq. (3), it is desirable to express the Wigner distribution function in terms of relatively narrow GPPs. Naturally this goes at the price of a relatively large number of packets. The requirement of spatial confinement of the packets is for two different reasons. First of all, we want to limit the number of derivatives in the Taylor expansion of the potential energy function in a CLE propagation of GPPs. As will be shown below, the numerical integration will be most convenient if the potential is locally quadratic within the extension of each GPP. Furthermore, one of the key quantities to be determined in a quantum–classical (QCLE) propagation is the nonadiabatic transition probability. This quantity varies rapidly in the vicinity of avoided crossings of adiabatic potential energy surfaces which necessitates a relatively dense sampling.

Our *ansatz* for Gaussian phase-space packets can be written as[15,31]

$$w_n(R,P)=B_n \exp\left[-\begin{pmatrix} R-R_n \\ P-P_n \end{pmatrix}^T \mathbf{G}_n \begin{pmatrix} R-R_n \\ P-P_n \end{pmatrix}\right] \tag{7}$$

where B_n is the (positive or negative) amplitude of the nth GPP and where the real, symmetric, positively definite $2D \times 2D$ matrix G_n is given by

$$\mathbf{G}_n=\begin{pmatrix} \alpha_n & \beta_n \\ \beta_n & \gamma_n \end{pmatrix}. \tag{8}$$

The elliptic phase-space contour is determined by the real symmetric matrices $\alpha_n, \beta_n, \gamma_n$. In order to fit the linear superposition of the GPPs as closely as possible to the original Wigner distribution (3), we proceed as follows: Similar to the procedure for the GWP decomposition of the initial wave function described above, the centers of the GPPs are obtained by a Monte Carlo sampling of the regions of phase space where the absolute value of the quasiprobability density exceeds a certain threshold. Subsequently, the mean square deviation between the Wigner distribution and a superposition of GPPs,

$$\xi(M;w_n)=\sum_{k=1}^{K}\left|W(R_k,P_k)-\sum_{n=1}^{N} w_n(R_k,P_k)\right|^2 \tag{9}$$

has to be minimized for a set of K sampling points (R_k,P_k). When only the amplitudes B_n of the GPPs are to be fitted, the minimization of the error ξ reduces to a problem of linear optimization which is equivalent to the solution of the following system of linear equations

$$SB=W, \tag{10}$$

where vector W contains the values $W(R_k,P_k)$ of the Wigner distribution at the sampling points, vector B contains the unknown amplitudes B_n, and the elements of matrix S can be written as

$$S_{kn}=\exp\left[-\begin{pmatrix} R_k-R_n \\ P_k-P_n \end{pmatrix}^T \mathbf{G}_n \begin{pmatrix} R_k-R_n \\ P_k-P_n \end{pmatrix}\right]. \tag{11}$$

If we choose the set of sampling points identical to the centers of the GPPs, the matrix elements are equal to the overlaps of the GPPs. In general, this matrix is expected to be sparse and a variety of special algorithms can be used for the efficient solution of sparse linear systems.[32] It is noted that the linear problem (10) may become numerically ill conditioned for a large number of wide GPPs, N, whenever the function to be approximated significantly oscillates on length scales comparable to the width of the GPPs. However, this does not pose a severe problem since (1) it can be monitored by computing the condition number of matrix S, and (2) we can avoid the problem by reducing the widths of the GPPs.

In principle, one may consider to optimize the width parameters $\alpha_n, \beta_n, \gamma_n$, too. However, this would lead to a nonlinear system of equations. We anticipate that in practical simulations it is advisable to circumvent this difficulty even when the reduced flexibility of the individual GPPs will have to be compensated by an increased number of them. It is noted that the present representation correctly reproduces the Wigner distribution also in regions where it is negative indicating a nonclassical behavior. An example is given in Fig. 4

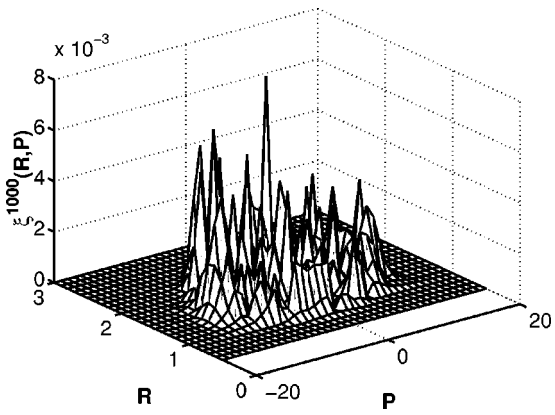

FIG. 4. Deviation of the Monte Carlo sampled Wigner distribution for $v=4$ eigenstate of the Morse oscillator [1000 Gaussian phase-space packets, optimized for $\epsilon=0.01$ in (9)] from known analytic results.

showing a decomposition of the Wigner distribution for the $v=4$ state of the Morse oscillator. Using 1000 GPPs the local error could be reduced to $\xi<0.01$.

III. CLASSICAL LIOUVILLE DYNAMICS

A. Equations of motion

Once a suitable representation of the initial density is available, we now intend to develop a numerical scheme for the dynamical problem. In the following we consider a conservative classical Hamiltonian

$$H=\tfrac{1}{2}P^T M^{-1} P+V(R), \tag{12}$$

where M is a $D\times D$ matrix containing the masses on the diagonal. Then the phase-space density is transported according to the classical Liouville equation

$$\partial_t W(R,P,t)=-M^{-1}P^T \boldsymbol{\nabla}_R W(R,P,t) + (\boldsymbol{\nabla}_R V(R))^T \boldsymbol{\nabla}_P W(R,P,t). \tag{13}$$

Inserting the definition of GPPs (7) into the above equation of motion (13), the evolution of the GPP parameters is readily obtained by collecting equal powers of $R-R_n$ and $P-P_n$,

$$\partial_t R_n = M^{-1}P_n, \tag{14a}$$

$$\partial_t P_n = -V^{(1)}(R_n), \tag{14b}$$

$$\partial_t \mathbf{G}_n = \mathbf{C}(R_n)\mathbf{G}_n+\mathbf{G}_n\mathbf{C}^T(R_n), \tag{14c}$$

where the $2D\times 2D$ dimensional matrix $\mathbf{C}$ is defined as

$$\mathbf{C}(R_n)=\begin{pmatrix} 0 & V^{(2)}(R_n) \\ -M^{-1} & 0 \end{pmatrix}. \tag{15}$$

Note that a locally quadratic potential energy function has been assumed, i.e., within the spatial extension of the packet, the potential can be represented by its gradient $V^{(1)}$ and the Hessian matrix $V^{(2)}$ only. Obviously, the evolution (14a)–(14b) of the vectors R,P is equivalent to Hamilton's equations of motion while the evolution (14c) of the matrices α,β,γ determining the shape of the GPPs is governed by the Hessian of the potential energy function. Hence, for a

D-dimensional configuration space, we have to deal with a system of $2D+3(D-1)D/2$ coupled linear, ordinary differential equations.[15,31]

Since classical and quantum-mechanical propagation coincide for harmonic potentials, the above GPP dynamics (14) represents a direct phase-space analogue to Heller's celebrated ''thawed'' GWP dynamics.[27] A generalization to overcome the restriction to locally quadratic potentials is in principle possible, e.g., by including higher order terms inside the exponential of (7) and/or considering polynomial prefactors. Apart from losing the simplicity of the above equations of motion, such approaches always involve higher derivatives of the potential energy function and, hence, a combinatorial growth of the effort to calculate all mixed derivatives. Instead, a practical alternative would be to monitor the widths of the wave packets during propagation. If one of them exceeds a certain threshold given by a typical length scale of the potential, it may be advisable to suspend the propagation and to refit the current distribution by a new set of GPPs by minimizing (9). Thus, the extra width can be compensated by an increased amplitude of neighboring GPPs and the locally quadratic approximation of the potential energy surface can always be fulfilled with desired precision.

B. Expectation values

The most elementary expectation value to be considered is the ''volume'' of the individual GPPs in phase space,

$$Z_n = \int\int w_n(R,P)\,dR\,dP = \frac{B_n \pi^D}{\sqrt{\det \mathbf{G}_n}} \tag{16}$$

which is invariant under the above evolution (14). Hence, the total volume, $Z=\Sigma_n Z_n$, remains unity for all times thus ensuring conservation of probability. Other important formulas are the expressions for the expectation values of kinetic and potential energy. After some tedious manipulations one obtains the following expressions:

$$\begin{aligned}\langle T\rangle &= \sum_n \int\int \tfrac{1}{2} P^T M^{-1} P\, w_n(R,P)\,dR\,dP \\ &= \sum_n (\tfrac{1}{2} P_n^T M^{-1} P_n + \mathrm{tr}(\mathbf{F}_n^{-1}\mathbf{K}_n)) Z_n, \end{aligned} \tag{17}$$

$$\begin{aligned}\langle V\rangle &= \sum_n \int\int V(R)\, w_n(R,P)\,dR\,dP \\ &= \sum_n (V^{(0)}(R_n) + \mathrm{tr}(\mathbf{F}_n^{-1}\mathbf{L}_n)) Z_n, \end{aligned} \tag{18}$$

where the first term on the right-hand side stands for the kinetic or potential energy calculated at the centers (R_n,P_n) of the GPPs in momentum or position space, respectively. The influence of the finite width of the packets is reflected in the second term characterized by the $2D\times 2D$ matrices

$$\mathbf{K}_n = \tfrac{1}{2}(U_n^{(1)}U_n^{(2)})^T M^{-1}(U_n^{(1)}U_n^{(2)}), \tag{19}$$

$$\mathbf{L}_n = \tfrac{1}{4}(U_n^{(3)}U_n^{(4)})^T V^{(2)}(R_n)(U_n^{(3)}U_n^{(4)}), \tag{20}$$

and the diagonal matrices, $\mathbf{F}_n$, containing the eigenvalues of the shape parameter matrices $\mathbf{G}_n$. The corresponding eigenvectors are arranged in a blockwise manner

$$\mathbf{U}_n = \begin{pmatrix} U_n^{(1)} & U_n^{(2)} \\ U_n^{(3)} & U_n^{(4)} \end{pmatrix}. \tag{21}$$

In the limit of infinitely narrow GPPs the reciprocal eigenvalues F^{-1} are converging towards zero and the expressions for the expectation values (17) and (18) are converging towards those obtained from an ensemble of classical trajectories.

C. Numerical integrator

Next, a fast and efficient integrator for classical Liouville dynamics shall be constructed. We proceed in analogy to the derivation of integrators in classical molecular dynamics in terms of Lie generators. First we rewrite the above set of coupled equations (14) as

$$\dot{z} = i\hat{\mathcal{L}} z, \tag{22}$$

where z is a generalized vector containing $R,P,\mathbf{G}$ and where $\hat{\mathcal{L}}$ is the Lie-generator corresponding to the right-hand side of evolution (14). Then a formal solution is simply given by

$$z(\tau) = \exp(i\tau\hat{\mathcal{L}}) z(0). \tag{23}$$

As a next step, the Lie generator $\hat{\mathcal{L}}$ can be decomposed into $\hat{\mathcal{L}}=\hat{\mathcal{L}}_1+\hat{\mathcal{L}}_2$ where $\hat{\mathcal{L}}_1$ is the Lie generator describing the evolution (14a) of the GPP centers in configuration space, R_n, while $\hat{\mathcal{L}}_2$ is the Lie generator for Eqs. (14b) and (14c) describing the evolution of P_n and $\mathbf{G}_n$. Under these conditions one can use a Strang-splitting[36] resulting in

$$e^{i\tau\hat{\mathcal{L}}} = e^{i\tau/2\hat{\mathcal{L}}_1} e^{i\tau\hat{\mathcal{L}}_2} e^{i\tau/2\hat{\mathcal{L}}_1} + o(\tau^3) \tag{24}$$

which results in the following numerical scheme (omitting GPP index n)

$$\begin{aligned} R(t_{1/2}) &= R(t_0) + \frac{\tau}{2} M^{-1} P(t_0), \\ P(t_1) &= P(t_0) - \tau V^{(1)}(R(t_{1/2})), \\ \mathbf{G}(t_1) &= e^{\tau \mathbf{C}(R(t_{1/2}))} \mathbf{G}(t_0) e^{\tau \mathbf{C}^T(R(t_{1/2}))}, \\ R(t_1) &= R(t_{1/2}) + \frac{\tau}{2} M^{-1} P(t_1), \end{aligned} \tag{25}$$

where t_0, $t_{1/2}$, and t_1 indicate the beginning, the middle, and the end of a timestep τ, respectively. Clearly this is a modification of the well-known leap-frog (or Verlet) algorithm frequently used in conventional molecular dynamics which is symplectic with respect to R_m and P_m. In addition, it can be shown that the phase space volume of GPPs as defined in (16) is conserved, too.

D. Example: Photodissociation

As an example for the application of the proposed dynamical scheme we consider a one-dimensional model of direct photodissociation of a diatomic molecule upon instan-

taneous excitation to a repulsive state. Typically, the excited state dynamics is very fast such that classical Liouville dynamics represent a good approximation to quantum dynamics.[19] However, there may be important quantum effects connected with the initial vibrational state. Such quantum effects are especially pronounced if the ground state is very shallow and/or if the molecule is initially vibrationally excited. In particular, the reflection principle states that the shape of the initial quantum-mechanical ground state density is reflected in the kinetic energy distribution (KED) of the photofragments.[18]

In our simulations we choose the first vibrationally excited state of a harmonic ground state potential with $\omega = 0.01$ centered at $R = 2.5$ for a (reduced) mass of $M = 1836$ (all numbers in atomic units). Upon instantaneous excitation of the electronic system by an ultrashort light pulse the nuclear dynamics is governed by a steeply repulsive excited state potential $V(R) = 1/R$ leading to fast separation of the photofragments. Three different approaches to the numerical solution of the CLE (13) are compared: The traditional approach using (weighted) classical trajectories represents the limit of infinitely narrow GPP distributions in phase space where the trajectory results have been sorted into 20 equally spaced bins (bars). This is contrasted with the finite width GPPs as described above where the KED can be calculated analytically (circles). In either case, the equations of motion are solved by the (modified) leap-frog integrator given in (25) for 45, 100, and 400 trajectories or GPPs. For comparison we also calculated a KED using a grid-based method (512×512 points, curve) where the partial derivatives are evaluated by means of fast Fourier transforms and where the time propagation is performed by means of a split operator scheme.

Figure 5 illustrates the kinetic energy distribution (KED) at an arbitrarily chosen time ($t = 400$) during the dissociation process. The GPP-based solution practically coincides with the (numerically exact) grid-based solution, even for relatively few GPPs ($N = 45$). The trajectory based solution, however, shows severe deviations. First of all, the high energy tail of the spectrum is missing for $N = 45,100$ because there are no trajectories in the Monte Carlo set which sample the initial densities at the very largest values of R. Although the GPP centers are based on the same pseudorandom numbers, the finite widths of the GPPs serve to correctly reproduce the tail of the spectrum. Second, the trajectory based solution produces negative values near the minimum of the KED. This artifact persists also for a relatively large number of trajectories ($N = 100$) while it barely exists for the GPP solution. In summary, the propagation of finite width GPPs gives a much more faithful representation of classical Liouville dynamics than the conventional propagation of trajectories.

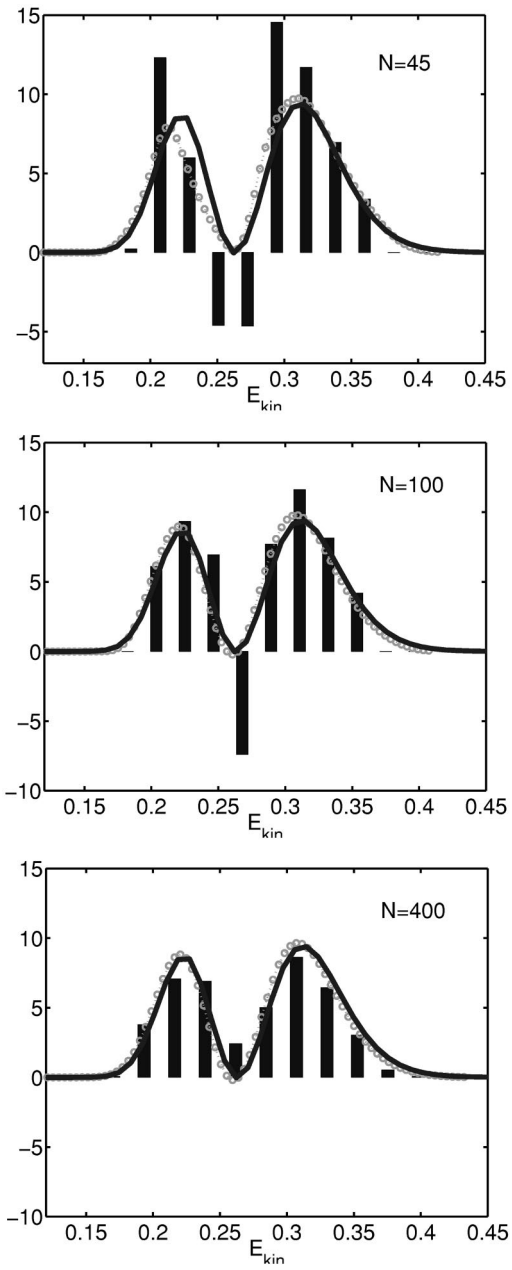

FIG. 5. Kinetic energy distribution upon photodissociation of a vibrationally excited diatomic molecule. Numerical solution of the classical Liouville equation by propagation of (weighted) ''delta'' trajectories (bars) and by propagation of Gaussian phase-space packets (circles) for three numbers N of trajectories or packets. For comparison, the solid curve shows a grid-based solution of the Liouville equation.

IV. CONCLUSION

The present work mainly addresses two open questions in the methodology of classical Liouville dynamics of multidimensional systems. The first part of the paper deals with the proper incorporation of quantum initial conditions in terms of an initial Wigner quasidistribution function. To this end, a novel scheme for the decomposition of a wave function into Gaussian wave packets has been proposed as an efficient means of performing a numerical Wigner transform. The Monte Carlo based technique is especially suitable for highly-dimensional problems where grid-based FFT methods are prohibitive because of the exponential scaling of the numerical effort. In contrast to most previous numerical studies of photoinduced dynamics, this technique is not restricted to the special case of a multidimensional Gaussian wave function where the Wigner distribution function is known to be positive. Consequently, we expect the future potential of the proposed method, e.g., for strongly anharmonic and corre-

lated vibrational molecular states. Apart from the use of variational calculations, stationary multidimensional wave functions can be obtained from, e.g., quantum Monte Carlo[37] or vibrational self-consistent-field simulations.[38]

The second part of the present work deals with classical Liouville dynamics. As an intermediate step, the Wigner quasidistribution function is sampled by a number of relatively narrow Gaussian phase-space packets (GPPs) in a Monte Carlo procedure. This allows a simple and efficient solution of the classical Liouville equation within the approximation of locally quadratic potentials. In contrast to the usual representation in terms of δ-like particles (trajectories) and classical Hamiltonian transport, the novel scheme offers two major advantages. First, it improves the sampling of phase space, thus permitting to employ a relatively low number of packets. However, this goes at the expense of calculating second derivatives of the potential energy surface. Second, the GPP dynamics can be used where a faithful, i.e., a dense representation of phase-space functions is required. This is the case, e.g., for the nonadiabatic dynamics of a system of light and heavy particles governed by the quantum-classical Liouville equation.[13]

ACKNOWLEDGMENT

Financial support by the *Deutsche Forschungsgemeinschaft* through program SFB 450 ''Analysis and control of ultrafast photoinduced reactions'' is gratefully acknowledged.

[1] E. P. Wigner, Phys. Rev. **40**, 749 (1932).
[2] M. Hillery, R. F. O'Connell, M. O. Scully, and E. P. Wigner, Phys. Rep. **106**, 121 (1984).
[3] H.-W. Lee, Phys. Rep. **259**, 147 (1995).
[4] W. P. Schleich, *Quantum Optics in Phase Space* (Wiley–VCH, Berlin, 2001).
[5] O. Prezhdo and V. V. Kisil, Phys. Rev. A **56**, 162 (1997).
[6] C. C. Martens and J.-Y. Fang, J. Chem. Phys. **106**, 4918 (1997).
[7] P. Gerard, P. A. Markowich, N. J. Mauser, and F. Poupaud, Commun. Pure Appl. Math. **50**, 323 (1997).
[8] R. Kapral and G. Ciccotti, J. Chem. Phys. **110**, 8919 (1999).
[9] C. Schütte, Konrad–Zuse–Center, Preprint SC-99-10, 1999, available through http://www.zib.de/bib
[10] A. Donoso and C. C. Martens, J. Chem. Phys. **112**, 3980 (2000).
[11] M. Santer, U. Manthe, and G. Stock, J. Chem. Phys. **114**, 2001 (2001).
[12] I. Horenko, B. Schmidt, and C. Schütte, J. Chem. Phys. **115**, 5733 (2001).
[13] I. Horenko, C. Salzmann, B. Schmidt, and C. Schütte (unpublished).
[14] C.-C. Wan and J. Schofield, J. Chem. Phys. **116**, 494 (2002).
[15] J. Ma, D. Hsu, and J. E. Straub, J. Chem. Phys. **99**, 4024 (1993).
[16] A. Donoso and C. C. Martens, Phys. Rev. Lett. **87**, 223202 (2001).
[17] R. N. Porter and L. M. Raff, in *Dynamics of Molecular Collisions*, edited by W. H. Miller (Plenum, New York, 1976), pp. 1–52.
[18] R. Schinke, *Photodissociation Dynamics* (Cambridge University Press, Cambridge, 1993).
[19] R. B. Gerber, A. B. McCoy, and A. Garcia-Vela, Annu. Rev. Phys. Chem. **45**, 275 (1994).
[20] M. Hug, C. Menke, and W. P. Schleich, J. Phys. A **31**, 217 (1998).
[21] M. Hug, C. Menke, and W. P. Schleich, Phys. Rev. A **57**, 3188 (1998).
[22] M. Hug, C. Menke, and W. P. Schleich, Phys. Rev. A **57**, 3206 (1998).
[23] R. L. Hudson, Rep. Math. Phys. **6**, 249 (1974).
[24] A. Szabo and N. S. Ostlund, *Modern Quantum Chemistry* (Macmillan, New York, 1982).
[25] M. J. Davis and E. J. Heller, J. Chem. Phys. **71**, 3383 (1979).
[26] S. Garashchuk and J. C. Light, J. Chem. Phys. **114**, 3929 (2001).
[27] E. J. Heller, J. Chem. Phys. **62**, 1544 (1975).
[28] E. J. Heller, Acc. Chem. Res. **14**, 368 (1981).
[29] D. Huber, E. J. Heller, and R. G. Littlejohn, J. Chem. Phys. **89**, 2003 (1988).
[30] M. A. Sepulveda and F. Grossmann, Adv. Chem. Phys. **96**, 191 (1996).
[31] S. Mukamel, *Principles of Nonlinear Optical Spectroscopy* (Oxford University Press, New York, 1995).
[32] W. H. Press, S. A. Teukolsky, W. T. Vetterling, and B. P. Flannery, *Numerical Recipes in Fortran* (Cambridge University Press, Cambridge, 1992).
[33] W. H. Zurek, Phys. Today **44**, 36 (1991).
[34] H.-W. Lee and M. O. Scully, J. Chem. Phys. **77**, 4604 (1982).
[35] J. P. Dahl and M. Springborg, J. Chem. Phys. **88**, 4535 (1988).
[36] G. Strang, SIAM (Soc. Ind. Appl. Math.) J. Numer. Anal. **5**, 506 (1968).
[37] J. B. Anderson, Int. Rev. Phys. Chem. **14**, 85 (1995).
[38] G. M. Chaban, J. O. Jung, and R. B. Gerber, J. Chem. Phys. **111**, 1823 (1999).